

# Essential dynamics of the cold denaturation: pressure and temperature effects in yeast frataxin

Yanis R. Espinosa,¹ J. Raúl Grigera,¹,² and Ernesto R. Caffarena³\*

#### ABSTRACT

The cold denaturation of globular proteins is a process that can be caused by increasing pressure or decreasing the temperature. Currently, the action mechanism of this process has not been clearly understood, raising an interesting debate on the matter. We have studied the process of cold denaturation using molecular dynamics simulations of the frataxin system Yfh1, which has a dynamic experimental characterization of unfolding at low and high temperatures. The frataxin model here studied allows a comparative analysis using experimental data. Furthermore, we monitored the cold denaturation process of frataxin and also investigated the effect under the high-pressure regime. For a better understanding of the dynamics and structural properties of the cold denaturation, we also analyzed the MD trajectories using essentials dynamic. The results indicate that changes in the structure of water by the effect of pressure and low temperatures destabilize the hydrophobic interaction modifying the solvation and the system volume leading to protein denaturation.

Proteins 2016; 00:000–000. © 2016 Wiley Periodicals, Inc.

Key words: cold denaturation; hydrophobic interaction; water structure; essential dynamics; molecular dynamics.

# INTRODUCTION

Protein cold denaturation, the transition from folding-unfolding (F-U) as a consequence of decreasing the temperature as well as the increasing of pressure, is a property of globular proteins. 1-5 The study of the cold denaturation is crucial for understanding the determining forces of protein folding. However, the elucidation of this process is still under debate.<sup>2,4,5</sup> A sensible explanation can be given by the Gibbs-Helmholtz approach, which considers the diminishing of hydrophobic interaction resulting in the hydration of non-polar groups at low temperature. 1-3 Moreover, the F-U transition occurs at a temperature below 0°C, where most aqueous solutions are frozen, hindering the study of the cold denaturation. Because of this experimental studies have normally been done by altering physiological conditions either by changing the pH, adding chemical denaturing agents, submitting the protein to high pressures or inserting special mutation agents. 1,6 Consequently, extrapolation from results based on artificial denaturation to states under physiological conditions is difficult to correlate.<sup>7</sup>

Experimental evidence reinforces the importance of the solvent in the F–U protein transitions, revealing that the greatest contribution to the F–U free energy,  $\Delta G = G_{\rm U} - G_{\rm F}$ , is mostly determined by its structure.  $^{2,5-8}$  In structural folding of aqueous-soluble proteins, nonpolar amino acids in a native protein are organized in a spatial distribution that facilitates the formation of a hydrophobic core aiming at minimizing the exposure to the water. This effect was named by Kauzmann<sup>9</sup> as hydrophobic interaction. This new concept opens to debate whether the stability of proteins is caused by van der Waals interactions between nonpolar chains, or if water induces the formation of the nonpolar core. <sup>10</sup> In this regard, Privalov claims that the hydrophobic interaction is a combination both processes. <sup>2</sup>

Additional Supporting Information may be found in the online version of this

\*Correspondence to: Ernesto R. Caffarena; Fundação Oswaldo Cruz., Rio de Janeiro, Programa de Computação Científica (PROCC), CEP, 21040-360 Rio de Janeiro, Brazil. E-mail: ernesto@fiocruz.br

Received 21 July 2016; Revised 19 October 2016; Accepted 25 October 2016 Published online 00 Month 2016 in Wiley Online Library (wileyonlinelibrary. com). DOI: 10.1002/prot.25205

© 2016 WILEY PERIODICALS, INC.

<sup>&</sup>lt;sup>1</sup> CEQUINOR (CONICET-UNLP), 120 e/61 y 62, Universidad Nacional de La Plata, La Plata 1900, Argentina

<sup>&</sup>lt;sup>2</sup> Departmento de Biología, Facultad de Ciencias Exactas, Universidad Nacional de La Plata, La Plata 1900, Argentina

<sup>&</sup>lt;sup>3</sup> Fundação Oswaldo Cruz., Rio de Janeiro, Programa de Computação Científica (PROCC), CEP, 21040-360 Rio de Janeiro, Brazil

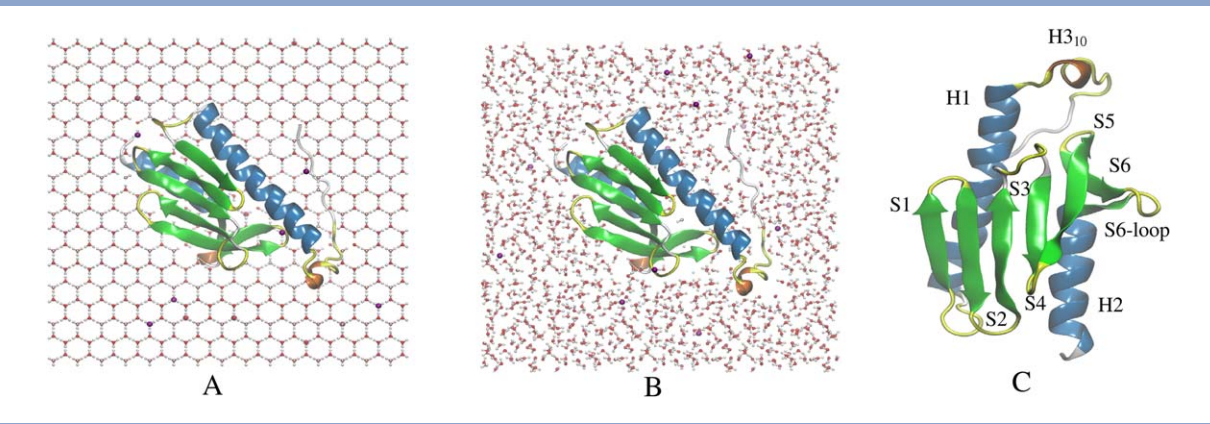


Figure 1 Initial configurations for the MD simulations. In A, frataxin immersed in Ice  $I_h$ . In B, frataxin in the liquid water state. This configuration was used as starting systems for 215, 293, and 323 K at 1 bar, and for the simulations under high pressure (3 kbar) and pressure scaling of 1–3000 bar (see Table I). In C, NMR structure of Yfh1 frataxin. <sup>19</sup>

Furthermore, the mechanism of protein unfolding at low temperatures is explained based on the solvation of amino acids in the protein core, that is, a favorable enthalpy of hydration of polar and nonpolar groups.<sup>7</sup> However, Dias and collaborators<sup>11</sup> revealed that the energy due to the hydrogen bonds between the water molecules surrounding the nonpolar residues is higher than the corresponding to the interaction between water and the protein itself. Chara et al. 12 using Molecular Dynamics simulations, have analyzed water structure showing that at low temperatures and high pressures, the capacity of water to form hydrogen bonds is affected resulting consequently in denaturation. Experimental data based on FTIR spectrometer modified for highpressure<sup>13</sup> supports this interpretation.

Likewise, at low temperature, the effect of high pressure modifies the structure of water. When a protein is subjected to high pressure, the entropic gain of minimizing exposed nonpolar surfaces to the solvent decreases and consequently the hydrophobic interaction is lost with the eventual denaturation of the protein. However, one interesting point in cold denaturation of proteins under high pressures is referring to the volume change. In this case, it has been reported that during the unfolding of proteins the change in the volume is positive at low pressures 14-16 and negative at high pressures. 14 In contrast, the transfer of hydrophobic compounds from a hydrophobic solvent to water is accompanied by a significant negative volume change at low pressure, resulting in an increase in the specific volume when the process occurs at high pressures (positive volume). 14,16,17 This paradox in the magnitude and sign of the change in volume because of the action of pressure is known as the protein volume paradox. 18

In this work, we investigated the influence of temperature and pressure on the stability of frataxin Yfh1. Frataxin, a protein encoded by the FXN gene in humans,

is the first protein to be reported whose denaturation occurs naturally at 0°C6 and constitutes a suitable system to study hot and cold denaturation. The hypothesis is that cold denaturation would be the responsible for the decrease in the strength of the hydrophobic effect. Experiments of cold denaturation of Yfh1 were already reported in a nuclear magnetic resonance (NMR) study at temperatures above 0°C under physiological conditions and without the addition of destabilizing agents.<sup>6</sup> Furthermore, the comparison between the high- and low-temperature unfolded states was accomplished supported by valuable experimental information.<sup>7</sup> Also, molecular dynamics simulations (MD) and essential dynamics analysis (ED) were employed as suitable computational techniques for studying this process.

## **MATERIALS AND METHODS**

#### System description

We studied the cold denaturation of frataxin protein (Yfh1) of Saccharomyces cerevisiae. Experiments performed by nuclear magnetic resonance spectroscopy (NMR) indicated that frataxin is a negatively charged globular protein composed of 123 residues (PDB code 2GA5<sup>19</sup>). The first 18 residues from the N-terminal lack a defined structure although a 3<sub>10</sub>-helix can be attributed to the fragment between residues 12 and 15. The globular domain consists of two terminal  $\alpha$ -helices [residues 19-42 (H1) and 109-120 (H2)] parallelly oriented. The  $\beta$ -sheet region is composed of five antiparallel  $\beta$ -sheets organized as follows: residues 50-55 (S1), 60-65 (S2), 69-74 (S3), 79-84 (S4), and 88-94 (S5). Additionally, a sixth β-sheet comprehend residues 97-100 (S6) and is connected to the H2 loop helix through eight amino acids, called domain region S6-loop [Fig. 1(C)]. Residues 121–123 are disordered. 19

Table I Summary About the Different Simulation Systems for Frataxin

Systems	Temperature (K)	Pressure (bar)	Water distribution	Water phase	Simulation time (ns)
F <sub>1</sub>	215	1	Hexagonal	Solid	500
$F_2$	215	1	Random	Liquid	500
$F_3$	293	1	Random	Liquid	500
F <sub>4</sub>	323	1	Random	Liquid	500
$F_5$	293	3000	Random	Liquid	500
$P_{\rm s}$	293	Scaling <sup>a</sup>	Random	Liquid	310 <sup>a</sup>

<sup>&</sup>lt;sup>a</sup>Scaling from 1 to 3000 bar increasing 100 bar every 10 ns.

## **MD SIMULATIONS**

Molecular dynamics simulations were performed using the Gromacs 4.6.3 package.<sup>20</sup> The Gromos 54A7 forcefield<sup>21,22</sup> was employed to account for intermolecular interactions. In all MD simulations, the electrostatic interactions were calculated using the particle-mesh Ewald (PME) summation scheme.<sup>23</sup> van der Waals interactions have been computed within a cutoff of 1.0 nm. The LINCS<sup>24</sup> algorithm was used to constrain all covalent bonds. The MD integration time step was two femtoseconds.

Initial atomic coordinates were taken from the yeast frataxin solution structure deposited in the Protein Data Bank (PDB code 2GA5<sup>19</sup>). The protein was solvated in a cubic simulation box of dimensions X = Y = Z = 6.75 nm with 9630 SPC/E water molecules<sup>25</sup> and periodic boundary conditions were applied. Fifteen Na+ counterions were added to neutralize the system.

Initially, we simulated two systems at 215 K and 1 bar. In the first one, the protein was immersed in a box with water in solid state Ice  $I_h$  [Fig. 1(A)]. The second system was hydrated by adding randomly water molecules in the liquid state [Fig. 1(B)]. Additionally, we performed four simulations, organized as follows: (i) control system at 293 K and 1 bar; (ii) heat denaturation system, at 323 K and 1 bar; (iii) denaturation system under high pressure at 293 K and 3 kbar; and (iv) denaturation system under pressure scaling from 1 to 3000 bar, increasing pressure gradually in steps of 100 bar each. The configuration corresponding to frataxin in aqueous solution defined the initial atomic coordinates for these systems [Fig. 1(B); Table I].

Initially, all the systems were optimized following a two-stage energy minimization process. In the first one, we applied 5000 steps of steepest descent algorithm. The second minimization stage applied conjugate gradient algorithm until an energy gradient ≤10 kJ mol<sup>-1</sup> nm<sup>-1</sup> was achieved. During the minimization process, the atomic positions from backbone were restrained to their initial positions using a harmonic potential with a force constant of 1000 kJ mol<sup>-1</sup> nm<sup>-1</sup> in all Cartesian directions.

After the energy minimization, all the systems were equilibrated for 5 ns in the NVT ensemble at the corresponding temperatures, using the *V-rescale* thermostat<sup>26</sup> and applying position restraints. Afterward, the systems were simulated for more five ns in the NpT ensemble at 1 bar using the Parrinello–Rahman barostat.<sup>27</sup>

Finally, we removed the position restraints and simulated all the systems for 500 ns, except for the one submitted to pressure scaling that was simulated for 310 ns, in stages, increasing 100 bars every ten ns (see Fig. 1S in Supporting Information) according to the reference pressure (Table I).

For the analyses of our simulations, we removed the unstructured region of frataxin, ranging from residue 1-18, to minimize noise. This region presents random motions that overestimate the conformational fluctuation of the protein.

# **ESSENTIAL DYNAMICS ANALYSIS**

#### Principal component analysis (PCA)

The PCA method was applied to determine the principal components of the systems. The covariance matrix (C) with elements  $C_{ij}$  was calculated using only alpha carbons (Cα) from frataxin. Calculations were carried out over the total time of the trajectory (for  $P_s$  the entire trajectory was concatenated). Thus, each element of C was calculated according to <sup>28</sup>:

$$C_{ij} = \langle (q_i - \langle q_i \rangle)(q_j - \langle q_j \rangle) \rangle, \tag{1}$$

where  $q_i$  and  $q_i$  are the internal coordinates of atoms iand j and  $\langle \rangle$  represents the average over total instantaneous structures sampled during the simulations. Diagonalization of the covariance matrix (C) gives rise to the eigenvalues  $(\omega_i)$  and eigenvectors  $(p_i)$  that are related to the amplitudes and the directions of the motions, respectively. Molecular dynamics trajectory can be projected on the eigenvectors to determine the principal components (PC)  $p_i(t)$ , i = 1, ..., 3N.

The first few PCs typically describe collective and global motions of the system, defining the dimensionality of the essential subspace. We evaluated the quality of sampling performing Essential Dynamics analysis by computing the cosine content  $(c_i)$  of the principal component  $p_i$  as,

$$c_i = \frac{2}{T} \left( \int \cos(i\pi t) p_i(t) dt \right)^2 \left( \int p_i^2(t) dt \right)^{-1}, \tag{2}$$

where T is the total simulation time. The evaluation of the cosine contribution for the first two principal components is sufficient to give an accurate idea of the protein behavior. <sup>29</sup> Insufficient sampling results in high  $c_i$  values, indicating a random diffusion behavior. <sup>30</sup> Thus,  $c_i$  values close to one indicate large amplitude motions in the protein dynamics, that is, a characteristic of random motions. Interpretation without having in mind distinctive features of the energy landscape <sup>29,31</sup> is not advisable.

Therefore, the average cosine content for the two first principal component (PC1 and PC2) was calculated as a function of the trajectory length (and as a function of the pressure for the  $P_s$  system). So, the evaluation of convergence of the conformational sampling and changes that occurred during the MD<sup>30</sup> was facilitated. Likewise, we analyzed the sampling convergence by computing the root mean square inner product (RMSIP) [Eq. (3)] as a measure of similarity between subspaces, assuming that the essential subspace of each system was defined by the five eigenvectors with higher eigenvalues,

RMSIP=
$$\frac{1}{5} \left( \sum_{i=1}^{5} \sum_{j=1}^{5} (n_i \cdot v_j) \right)^{1/2}$$
, (3)

where  $n_i$  and  $v_j$  are the eigenvectors of the subspaces to be compared.

#### Free energy landscape

We represented the two-dimensional free energy landscape (FEL) (considering two different reaction coordinates  $q_i$  and  $q_j$ ), based on the joint probability distributions  $P(q_i,q_j)$  of the system. The likelihood of finding the system in a particular state is defined as:

$$G_{i,j} = -K_{\mathrm{B}} \,\mathrm{T} \,\ln \left[ \frac{P(q_i, q_j)}{P_{\mathrm{Max}}(q_i, q_j)} \right], \tag{4}$$

where i and j indicate indexes for coordinates  $q_i$  and  $q_j$ ,  $G_{i,j}$  is the free energy associated with the state (i, j),  $K_{\rm B}$  is the Boltzmann constant, T is the absolute temperature,  $P(q_i,q_j)$  is an estimate of the probability density function obtained from a histogram of the MD data and  $P_{\rm max}$   $(q_i,q_i)$  is the probability of the most probable state.

# **RESULTS AND DISCUSSION**

Based on the hydrophobic effect, which asserts the solvent structure surrounding the protein is crucial for the denaturation occur, we analyzed the structural changes frataxin underwent when it was immersed in hexagonal structured ice  $I_h$  ( $F_1$ ) type at the melting temperature (215 K for the SPC/E model).<sup>32</sup> Similarly, we also investigated protein behavior when it was embedded in the liquid water at 215 K ( $F_2$ ). Simulations at 293 K ( $F_3$ ) (experimental temperature of maximum stability<sup>8</sup>) and 323 K ( $F_4$ ) (experimental temperature of heat denaturation<sup>7</sup>) were also carried out. This last case was considered as examples of denaturation of frataxin at high temperatures. Finally, we inspected how frataxin behaved when it was subjected to high hydrostatic pressure, achieving the upper limit of 3 kbar ( $F_5$  and  $P_8$ , in Table I).

#### Structural analysis

To verify the effect of temperature and pressure on the overall structure of the protein, we monitored the root mean square deviation (RMSD) of backbone atoms [Fig. 2(A)] and the root mean square (RMS) of residues. These analyses allowed us to assess the structural divergence of the protein over the simulation time taking as reference the initial structure. The RMS is used to calculate the distance between structures from the deviation of atom—pair distances, grouping them in conformational states.

At the temperature of 215 K in  $F_1$ , the protein adopted a more stable conformation corresponding to RMSD values around 0.38 nm [Fig. 2(A)]. According to the distribution of pairwise RMSD distances, the protein visited four distinct populations, which were identified by the peaks of the curve at 0.11; 0.16; 0.19; 0.24 nm, away from the reference structure during the simulation [Fig. 2(B)].

The RMSD in  $F_2$  stabilized around 0.36 nm [Fig. 2(A)] with distribution values centered on two close populations near 0.09 and 0.13 nm [Fig. 2(B)], plus a small one, fuzzily defined, near 0.18 nm. This particular system also showed a lower distribution of RMS values (0.04–0.24 nm) when compared to the system in solid state  $F_1$  (0.04–0.34 nm). The reason why protein in  $F_1$  presented a higher fluctuation about the system  $F_2$  in the liquid state might be possibly ascribed to the melting transition (solid ice into liquid water) resulting in a disruption of the protein structure.

At 293 K, frataxin showed stable deviation values, reaching an RMSD value of 0.4 nm [Fig. 2(A)]. Analysis of the RMS values evidenced two populations defined at 0.14 and 0.22 nm [see Fig. 2(B)] that correlate well with the states of the higher probabilities of visiting time (see "Essential Dynamics Analysis").

The broad distribution of the RMS values, from 0.08 to 0.42 nm, were observed for the protein in aqueous

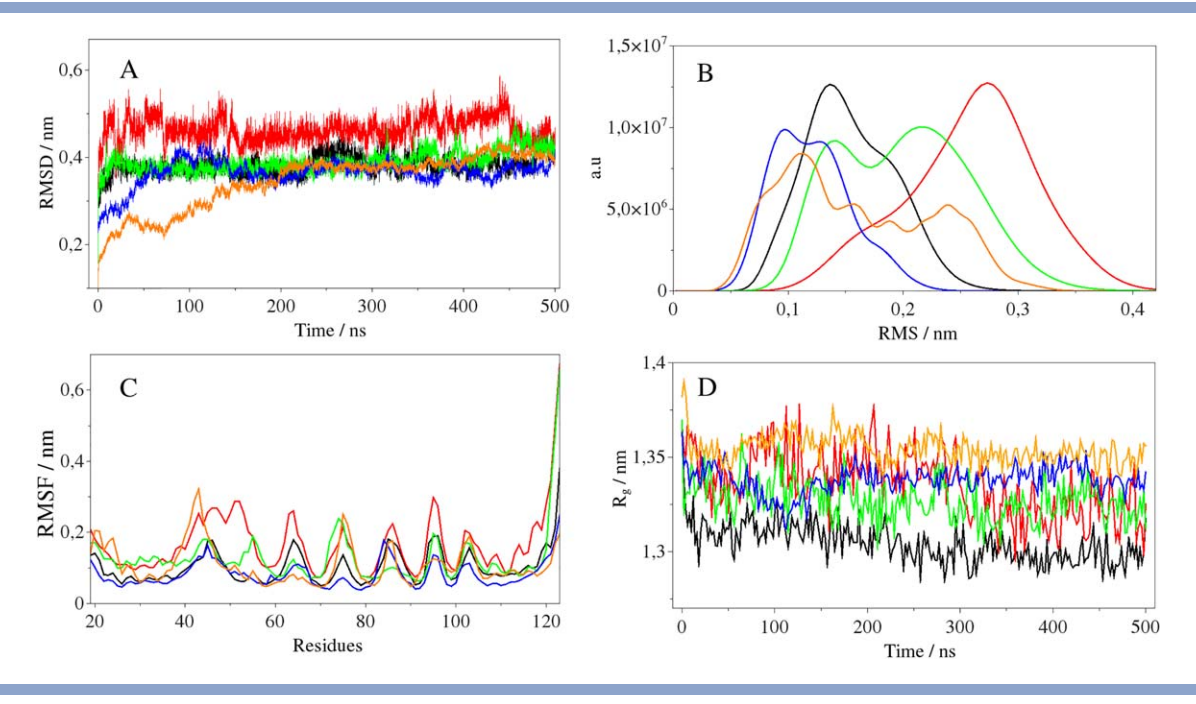


Figure 2 Structural and mobility analysis of frataxin. (A) Root mean square deviations (RMSD) was calculated aligning each of the systems with the NMR structure. (B) Distribution of pairwise RMSD distances computed in A. (C) Root mean square fluctuation (RMSF) per residue (starting from residue 19). (D) Radius of gyration ( $R_p$ ). In (A, B, and D) each of the calculations was performed taken into account the backbone atoms from frataxin. In (C), we use the alpha carbons. In orange, F1; blue, F2; green, F3; red, F4, and black F5. [Color figure can be viewed at wileyonlinelibrary.com]

solution at 323 K, with a sharp population at 0.28 nm and another less defined at 0.15 nm. The wide-ranging distribution can be attributed to the high number of states frataxin can adopt until achieving its stable conformation in water. According to the RMS, the RMSD analysis for this system showed the highest value, which oscillated around 0.48 nm with amplitude of 0.34 nm.

Finally, the system  $F_5$  under the high-pressure regime kept stable during the simulation, with an offset value of ~0.38 nm. This RMSD outcome was in agreement with the RMS values that showed the presence of a distinct group at 0.14 nm and a milder one at 0.19 nm.

On the other hand, the system  $F_3$  showed a thermal stability agreeing well with experimental evidence due to NMR and circular dichroism assays performed at this temperature.  $^{7,8}$  As expected, the system  $F_4$ , with the higher thermal disorder, presented the highest RMSD and RMS values. However, we observed a bias toward a well-defined configuration, similar to the one obtained at high pressures (the conformational populations seen in the RMS are analyzed in detail in the section "Free Energy Landscape").

Given the analysis above, we noted that the frataxin presented conformational variations depending on both temperature and pressure.

To check if the protein could lose structure due to the denaturing processes, we inspected the secondary structure content using definitions of the "Dictionary of Secondary Structure for Proteins" (DSSP).33 We found that the main structural elements did not show a significant loss of their secondary structure (see Table IS and Fig. 2S in Supporting Information) in the period the system was simulated.

# **Mobility analysis**

Predictably, the mobility of atoms in the protein increases in direct proportion to the temperature.

Furthermore, it is well known that freezing water through an MD is not possible. However, the opposite effect can be easily simulated and analyzed to detect the coexistence of states in water (solid-liquid), and inspect perturbations caused in the protein structure when ice melts.

Therefore, we compared the root mean square fluctuation (RMSF) of the C-α atoms of each frataxin residue for the five simulated conditions [Fig. 2(C)].

We observed that the fluctuation pattern for frataxin in  $F_1$  was higher than expected, beating the system  $F_2$  in liquid water.

Nevertheless, residues 28-38 located at the N-terminal H1 presented low fluctuations, showing a trend to maintain their structure in  $\alpha$ -helix, although residues 40–42, located at the C-terminal H1, showed the highest fluctuations. The binding region loop S1-H1 showed the highest fluctuation values for  $F_1$ . For the structures in β-sheet, S3 evidenced the highest mobility followed by S4 and, S5. In H2, the C-terminal region showed the highest fluctuation.

Comparing these results with the ones corresponding to  $F_4$ , we observed an increase in the fluctuation of H1, encompassing a 20-residue region (34–54) extending through S1. Also, S1 showed high fluctuations for residues 50–55, evidencing a tendency to lose the  $\beta$ -sheet structure. Likewise, S2, S3, S4, and S5, had greater mobility at the C-terminal region, in direct contact with the turns binding of  $\beta$ -sheets. Finally, the region H2 presented a growing mobility from the C-terminal to the N-terminal, indicating possibly a tendency to denaturation. Note that the region between residues 120–123, the terminal residues remained unstructured and consequently highly flexible, resulting in significant fluctuation values, especially for the systems presenting high thermal mobility.

The results observed in our simulations, for high and low temperatures, corroborated the experimental data<sup>6,7</sup> where frataxin at low temperatures showed a tendency to form and maintain  $\alpha$ -helices in H1, while at high temperatures this region did not preserve its local structure. However, at both temperatures 0 and 50°C, there is a greater persistence of H2 of remaining structured relative to H1, in agreement with our simulations. Moreover, although it can be seen experimentally that the  $\beta$ -sheet structures are fully deployed at 0 and 50°C, in our simulations this trend was more evident in  $F_4$ , where S1 displayed high RMSF values for all its residues. Nonetheless, all  $\beta$ -sheets in  $F_4$ , except in the S6-loop, showed high RMSF values in their C-terminal residues. In  $F_1$ , this trend was evident only for S3 and S4.

At 293 K, the system remained stable, with an increase in RMSF for residues located in the C-terminal S3 (residues 120–123) mainly due to thermal fluctuations that produced great mobility of this region. Meanwhile, for  $F_2$ , the fluctuation patterns presented low RMSF values, similar to H1 and S1 regions for the system  $F_5$ . When analyzing system  $F_5$ , it is clear that the increased pressure restricted the residue mobility of the protein. Interestingly, residues ranging from 19 to 60 exhibited a pattern of similar fluctuation to  $F_2$ . However, the system  $F_5$  tended to be slightly more fluctuating, being the C-terminal binding turns S2, S3, S4, and, S5 responsible for the greater fluctuations.

So far, our analysis suggests that residues located in  $\beta$ -sheet regions presented some similar behavioral patterns for the various simulated conditions but  $\alpha$ -helices tended to show different patterns. Additionally, we analyzed the radius of gyration  $(R_g)$  of frataxin for each of the simulated conditions. We observed that  $R_g$  decreased with the increasing pressure [Fig. 2(D)], suggesting that the system at high pressures became more compact, resulting in the restriction of its mobility, also observed in RMSF values of the residues [Fig. 2(C)].

Furthermore, the high fluctuation in the  $R_{\rm g}$  value when frataxin was subjected to 323 K suggests that the system explored a wider range of conformational states.

Based on the observation of the  $R_{\rm g}$  variation over simulation time, it becomes clear that frataxin expanded at low temperatures. This effect has been particularly evident for the system immersed in Ice  $I_{\rm h}$ , with a  $R_{\rm g}$  value around  $\sim 1.35$  nm. In this line, our simulation results agree well with experimental data reported by Aznauryan *et al.*,  $^{34}$  where the  $R_{\rm g}$  of frataxin decreases with increasing temperature. Therefore, during heat denaturation, a collapse occurs in the protein structure producing a reduction in  $R_{\rm g}$  value while the expansion of the protein during cold denaturation regime handles for the increase in  $R_{\rm g}$ .

## Essential dynamics analysis

To better understand the important protein movements occurred in the simulations, we analyzed the trajectories of the  $C-\alpha$  atoms from frataxin using principal component analysis (PCA). Thus, it was possible to detail the direction and amplitude of movements involved in conformational changes of the protein,<sup>35</sup> describing its essential dynamics (ED).

To analyze how the system responded to the action of increasing pressure, we monitored its dynamical evolution. The starting configuration was the same [Fig. 2(B)] than the one in liquid water at 293 K but subjected gradually to the action of pressure in a range comprised between 1 bar and three kbar [ $P_s$  (see "Materials and Methods")].

After the calculation of the eigenvalues, we were able to obtain the individual contribution for each principal component (PC) to the overall fluctuation in the protein (Supporting Information Fig. 3S). For the analysis, we selected the top five components with largest amplitudes, representing 82% of the movements for  $F_1$ , 65% for  $F_2$ , 66% for both  $F_3$  and  $F_4$  at atmospheric pressure, 61% for  $F_5$  and finally 66% for the one subjected to increasing pressure,  $P_8$ . Interestingly, the first component for  $F_1$  system represented 61.12% of the movements in frataxin, being the highest value for this component when compared to the other remaining systems (Supporting Information Fig. 3S).

For obtaining the principal components that define our essential subspaces, we calculated the projections of each trajectory onto their first five eigenvectors. For all the systems, except  $P_s$ , PC1 exhibited fluctuations in their residues that correlated very well with RMSF values. However, it is noteworthy that (i) the fluctuation of residues in the first  $\alpha$ -helix in  $F_1$  was the largest about the other systems and (ii) the first two PCs were responsible for the highest atomic fluctuations (Fig. 4S, Supporting Information). For the system  $P_s$ , no major fluctuation was found in any of the five PCs examined. In this particular case, the increased pressure restricted the mobility of atoms, as shown for the system  $F_5$ . Unfortunately, the

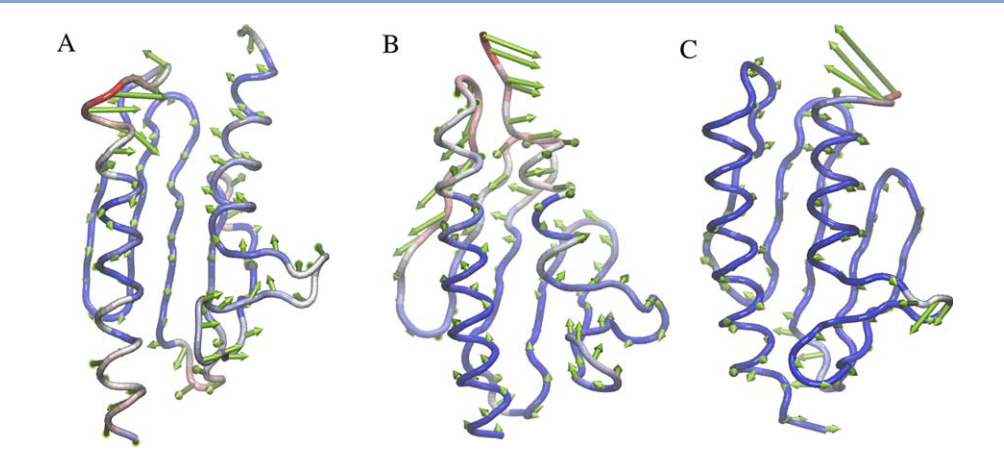


Figure 3 View of the direction and scope of the essential movements for frataxin  $(C\alpha)$  for the first PC at (A) low temperature, (B) high temperature, and (C) high pressure. [Color figure can be viewed at wileyonlinelibrary.com]

lack of experimental outcomes prevented us from performing analysis of possible structural changes of frataxin beyond these conditions.

Therefore, we focused the analysis of the essential movements on the first two PCs, responsible for most of the atomic fluctuations.

As a quality control of the ED analysis, we computed the cosine content for the two PCs. The cosine content was low for all simulation systems confirming that the motions described by the first components represented well the conformational transitions (Fig. 5S, Supporting Information).

Because the  $P_s$  system had a different time scale and it suffered from the influence of an increasing pressure during the simulation time, we analyzed the cosine content of this system separately. The PC1 first cosine content started to increase at approximately 700 bars (Fig. 6S, Supporting Information). Then, after reaching 1700 bars, the cosine content rose again until achieving its maximum (0.50) at 2300 bar. These values suggest that frataxin underwent two transitions, being the first previous to 1000 bar and the second one after 2000 bar, correlating well with variations in the behavior of  $R_{\alpha}$ [Fig. 6(B), Supporting Information]. Similarly, the  $R_g$ variation showed that the protein experienced both compression and expansion processes due to increasing values of pressure.

Finally, the cosine content analysis provided information on conformational changes during MD, indicating that the simulation times are optimal to ensure the convergence of collective structural movements.<sup>30,31</sup>

#### **Essential motions**

We analyzed leading movements by projecting the trajectories on the two first components PC1 and PC2

(Fig. 7S, Supporting Information) for each simulated condition. In a glimpse, we noted that movements for the first two components were different for every system (see Fig. 3 and Fig. 7S, Supporting Information). However, these motions presented a trend related to the closing and opening of the structures and, to the rotation of their helices.

For a better description of the direction and length of motions for every system, as well as the correlation between its subspaces, we estimated the overlapping of the first five principal components defining the essential subspace. These eigenvectors, corresponding to the largest eigenvalues, were evaluated by computing the root mean square of the intern product (RMSIP) of each trajectory. According to our analysis, we observed that there was no correspondence between each of the first five PCs for systems at low temperatures, high temperatures or high pressure, that is, the simulated systems showed no overlapping at all over PC1 (orthogonal eigenvectors) (Table IIS, Supporting Information). Hence, we suspect that under different conditions of temperature and pressure, intrinsic collective movements of the protein structure do not govern denaturing kinetics of frataxin. However, some PCs between systems showed overlap with values  $\geq 0.5$  (Table IIS, Supporting Information), for example, PC2 in  $F_5$  with PC3 in  $F_2$ ; PC1 and PC2 in  $F_3$  with PC2 in  $F_5$ ; PC5 in  $P_s$  with PC2 in  $F_1$  (to take some examples), indicating perhaps global patterns of correlated movements.

Particularly, at low temperatures, we observed that frataxin in Ice Ih did not result in RMSIP values higher than 0.5 with any other system. Furthermore, all systems (except  $F_1$ ) presented overlapping above 0.5 with  $F_3$ , proposing that systems experience similar movements to the reference system  $(F_3)$  and that denaturation kinetics can be characterized by opening and closing of the global

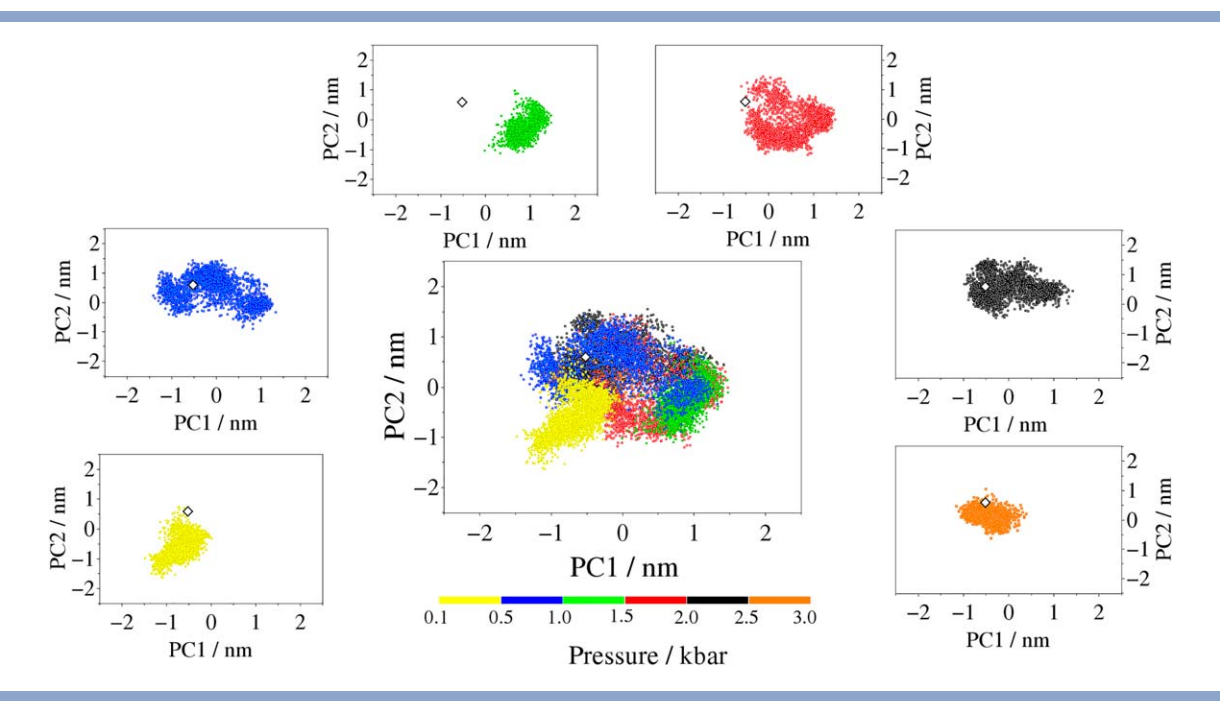


Figure 4

Bidimensional projection (2D) of the trajectory coupled to increased pressure within the first two PCs. Each point represents a transitional protein conformer adopted in each pressure. White diamonds show the original structure by NMR. The color coding represents the range in the increased pressure. Smaller boxes indicate protein substates for each pressure range analyzed. [Color figure can be viewed at wileyonlinelibrary.com]

structure and the rotational motion of the helices. This behavior was not apparent in the reference simulation and, in turn, they were more noticeable in  $F_1$ , indicating that these movements are necessary to the denaturation of frataxin at low temperatures.

## Subspace PC1/PC2

To understand the conformational dynamics of frataxin, we projected MD trajectories onto PC1 and PC2 for all simulated systems according to their time sequence (Fig. 8S, Supporting Information). With the timeline, it is possible to understand the transitions between conformational states when compared with its original structure, elucidated by NMR assays. <sup>19</sup>

We observed that the conformational space sampled was different for each condition. For the system immersed in Ice  $I_h$ , frataxin explored a wider range of conformational states about simulations performed at 215 K in the liquid state, as shown in RMS [Fig. 2(B)]. Moreover, the system in Ice  $I_h$  visited different conformational states during the first 300 ns after which it achieved a broader vicinity of structures.<sup>3</sup>

When the frataxin was in aqueous solution at 293 K, the system explored the conformational space presenting close vicinity between conformations during the first 300 ns and then moved to the second group of structural conformations during the final 200 ns. With increasing temperature, at 323 K, the system scanned the conformational space

homogeneously, being extensive for the first 100 ns. This behavior is well correlated with results obtained through RMSD and  $R_g$  [see Fig. 2(A,D), respectively].

The high-pressure systems, at an invariant pressure of 3 kbar, the frataxin was initially away from its original configuration, returning to it after 300 ns. This effect is best seen in Figure 4, where frataxin was subjected to the effect of increasing pressure. Following  $R_{\rm g}$  variations [Fig. 6(B), Supporting Information], between 500 and 1000 bar, the frataxin moved away from its initial configuration, returning at configurations close to its native structure when pressure overcame the 2000 bar.

# Free energy landscape

During the trajectories, frataxin visited several states of the free energy landscape that could be assembled in different regions determined after the convergence was attained. Hence, the most likely distribution for the states was established to extract some thermodynamic properties. Thus, we analyzed the free energy landscape (FEL) taking the first two principal components obtained in the ED analysis as reaction coordinates.

When frataxin was immersed in Ice I<sub>h</sub>, we found that the protein explored conformational states that departed from their native structures (Fig. 8S, Supporting Information), revealing a gradual conformational transition toward a different state. After 300 ns, the system kept trapped in a local minimum, suggesting that ice structure

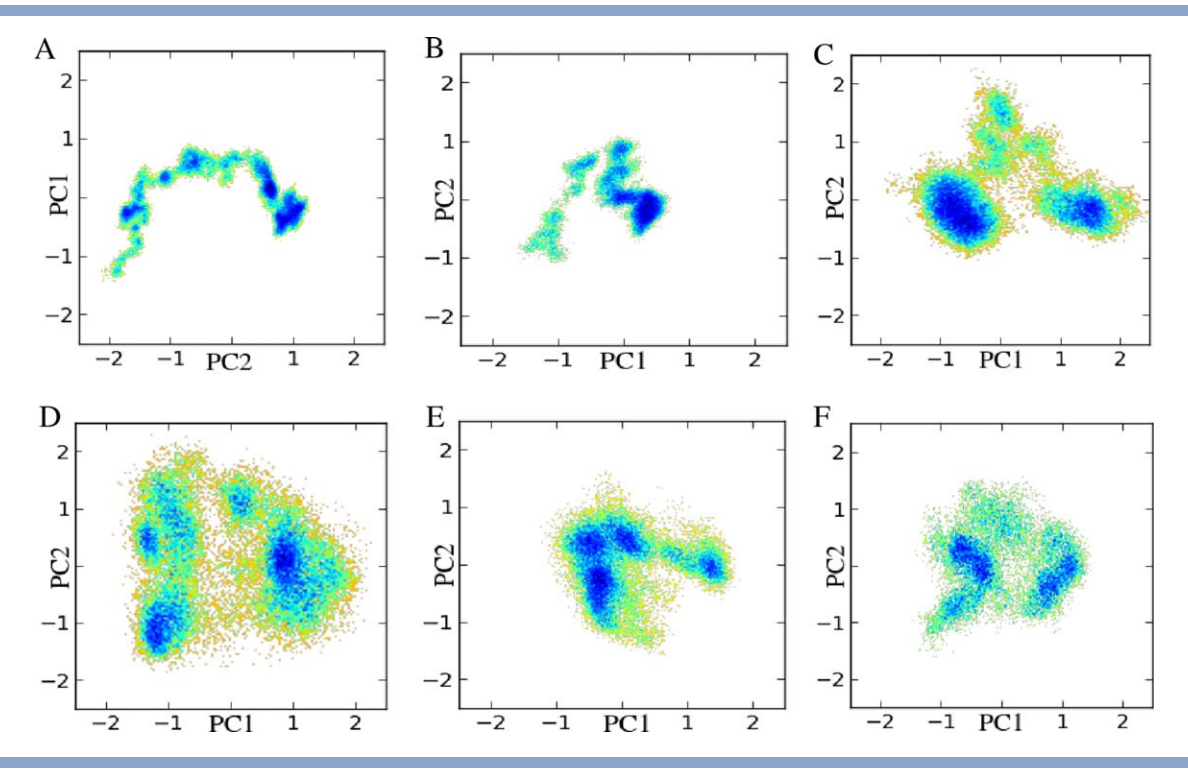


Figure 5 Free energy landscape (FEL) analysis using as reaction path the projections of frataxin Cα atoms trajectories onto the first two components. Free energy values are given in kcal mol<sup>-1</sup> indicated by the colour bar. Frataxin in (A), F<sub>1</sub>, (B) F<sub>2</sub>, (C) F<sub>3</sub>, (D), F<sub>4</sub>, (E) F<sub>5</sub>, and (F) P<sub>8</sub>. [Color figure can be viewed at wileyonlinelibrary.com]

caused an increasing perturbation in the frataxin structure and played an essential role in denaturation process at low temperatures (Fig. 8S, Supporting Information and Fig. 5). On the other hand, when frataxin was maintained at 215 K in aqueous solution, the system explored a more confined conformational space with fewer local minima.

By analyzing the trajectories of frataxin at 293 K, we observed that thermal fluctuations provoked transitions between two metastable states. With increasing temperature, at 323 K, the system jumped off of the minima and explored additional regions.

The systems that evolved under the action of high pressures, unlike of systems that experienced thermal denaturation, tend to return to configurations close to their native structure. Because in high-pressure regime (1.5–3.0 kbar) the conformational entropy decreased and the access to remote regions was not favored. However, the frataxin at low pressures (0.1-1.5 kbar) could visit energetically unfavorable remote regions, away from its native structure. High-pressure studies by NMR and crystallography in lysozyme and myoglobin, respectively, showed no significant differences (low RMSD values) between native structures and those denatured by high pressure. 15,36

Our analysis suggests that the exploration of frataxin to new conformations at low temperature can be

explained by the intensive activity characterized by opening and closing of the global structure and the rotational motions in their α-helices. As reported by Adrover et al., 6 H1 handles the collapse and maintenance of the secondary structure, where the C-terminal region is the most flexible one (Figs. 4S and 7S, Supporting Information). Moreover, the comparison between the essential subspaces for high and low temperatures showed that the systems responded in accordance to different denaturation kinetics (Table IIS, Supporting Information) as indicated by NMR result  $^7$ . Our result also shows that the high-temperature denaturation exerts a strong effect on H2 and β-sheets (especially S1). On the other hand, the kinetic of the protein denaturation by high pressure comprises partial deployment of the C-terminal regions of its  $\alpha$ -helices and expansion and contraction of the entire structure [Fig. 9(B), Supporting Information].

As a common and elucidative kinetic mechanism of protein unfolding process between cold and hot denaturation was not clearly revealed, we suppose that pressure and temperature effects on water structure might drive the natural movements of the protein. With this in mind, we computed the solvent-accessible surface area (SASA) for all systems [Fig. 6(A)] and found that the pressure caused a collapse in the native structure of the frataxin, mostly due to squeezing [Figs. 2(D),6(A), and 6S, Supporting Information]. Nevertheless, by analyzing

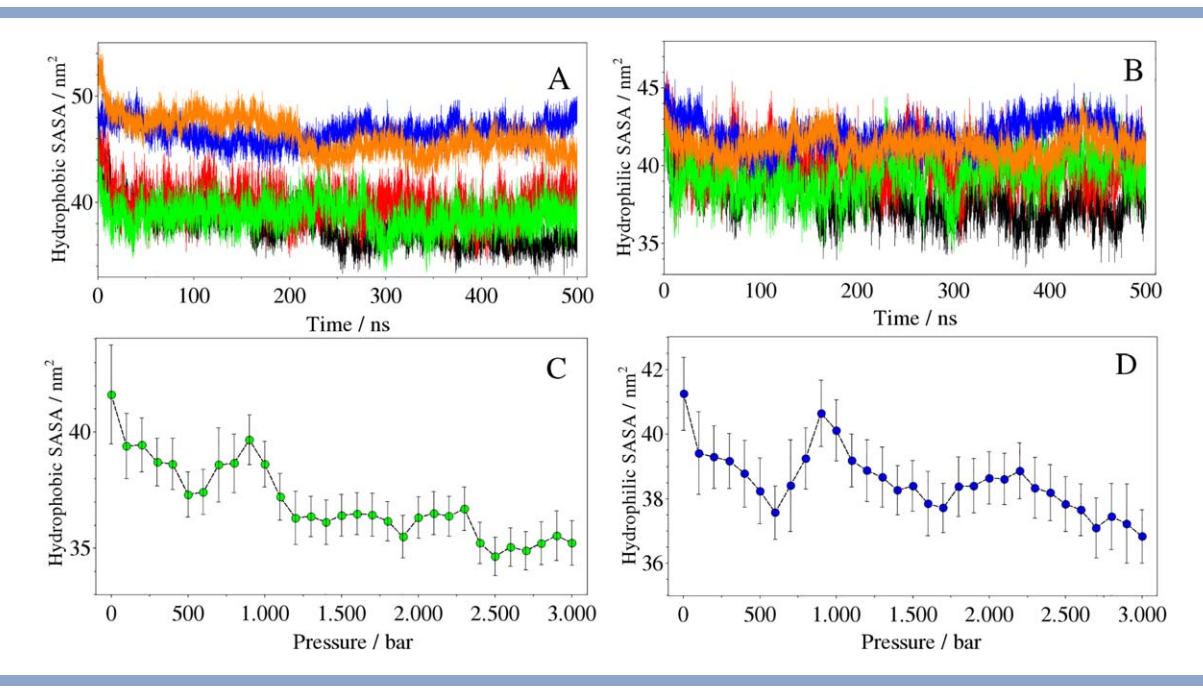


Figure 6 Solvent accessible surface area (SASA). In (A) hydrophobic and (B) hydrophilic SASA during 500 ns of trajectory. In orange, F1; blue, F2; green, F3; red,  $F_4$  and black  $F_5$ .In (C) hydrophobic and (D) hydrophilic SASA at pressure scaling ( $P_5$ ). Dots and error bars represent the average and standard deviations, respectively. [Color figure can be viewed at wileyonlinelibrary.com]

the conformational changes due to changes in pressure  $(P_s)$  [Fig. 6(C,D)] we perceived that in the low-pressure regime, up to 1000 bar, the hydrophilic and hydrophobic SASA were very close to their original values (considering standard deviation bars). With the increasing pressure, SASA value decreased reaching its minimum after 2300 bar (high pressure). Accordingly, the SPC/E water model at 2300 bar presents the low-density to highdensity transition, experimentally validated. 13 In both cases, the second coordination shell collapses on to the first coordination shell (See Fig. 10S, Supporting Information). Thus, two different local structures coexist, that is, an open tetrahedral structure [low-density (LDW)] and a more compact hexagonal one [high-density (HDW)]. 12,13 However, despite the theoretical approach of the SPC/E model, capable of representing the dynamic properties of water and the coexistence of two states, LDW and HDW in high pressure, the structural changes of the frataxin can only be validated by experiments.

Moreover, our results provide valuable information regarding the protein volume paradox. 18 Thus, at low pressures (~1 kbar) the increasing hydrophobic SASA can be directly related to positive volume change observed experimentally. 14,15 In this way, two phenomena coexist under high pressure. The first is the weakening of the hydrophobic effect at low pressures, allowing the exposure of hydrophobic residues, leading to an enhancement in volume; and the second has to do with the fact that when pressure increases the volume of the system decreases (negative volume<sup>14</sup>) due to higher compressibility.

The opposite effect was observed at low temperature, where hydrophobic SASA is maximum for all the simulated systems [see Fig. 6(A)]. This fact directly relates to the frataxin experimental reports where non-polar groups are exposed to water.<sup>6–8</sup>

# CONCLUSIONS

The frataxin model here studied allows a comparative analysis using experimental data, providing valuable information about the cold denaturation of proteins. Thus, according to ED analysis and the agreement with the experimental results, we were unable to detect a common kinetic mechanism of protein unfolding between cold and heat denaturation. However, increased activity in the unfolding kinetics is observed in αhelices.6-8

Our observations suggest that the cold and heat denaturations are driven because of changes in solvation of protein due to modifications in the water structure. At low temperature, we performed an MD simulation optimizing the hydrogen bonding interaction between water molecules, observing increments in the conformational entropic contribution of frataxin. In other words, the optimization of the H-bonds between solvent molecules leads to free movements of the proteins, suggesting the hydrophobic interaction is destabilized at low temperatures as a consequence of the changes in the water structure.<sup>5,12,17</sup> Hence, the inhibition of the hydrophobic

interaction along with the increasing hydration of nonpolar groups (increased hydrophobic SASA),<sup>2,5–7</sup> results in an enhancement of its volume reflected in the rise of its  $R_{\sigma}^{34}$ 

Likewise, when the frataxin was submitted to a low pressure (0.1-1.5 kbar), we observed a gradual inhibition of the hydrophobic interactions with the following exposure of the nonpolar residues, resulting in an increased of the volume of the frataxin ( $\Delta V$  positive). With a further increase of pressure, 1.5–3.0 kbar (high pressure) the frataxin was compacted decreasing its volume ( $\Delta V$  negative).

Our data support the idea that the contribution to positive  $\Delta V$  can be given by the exposure of the hydrophobic residues to the solvent, <sup>14</sup>, <sup>15</sup> due to the continuous inhibition process of the hydrophobic interaction regarding the changes in the water structure under pressure from a tetrahedral structure to a hexagonal one. 12 Thus, in the high-pressure regime, the surrounding solvent loses its structure, promoting protein compression until  $\Delta V$  becomes negative (decreased hydrophobic SASA).

Although it seems paradoxical that the volume change in protein denaturation becomes negative under high pressure, while hydrophobic compounds under these same conditions increase the specific volume, both processes are influenced by the hydrophobic effect. In a recently published study by MD simulations, we have shown that phase transitions produce positive volumes in these types of systems. This effect was proven in a computational model consisting in a micellar self-assembly with sodium dodecyl sulfate molecules. Structural changes, from spherical micelles at 1 bar to lamellar structures at high pressures, cause that enhance the system volume increase.<sup>37</sup> In summary, the shift in the sign and magnitude in volume will depend on the structural characteristics of each system. Finally, we can conclude that the cold denaturation of proteins and the SASA changes in high pressure are driven by the decrease of the hydrophobic effect because of the changes in water structures.

## **ACKNOWLEDGMENTS**

YRE thanks to Dr. Mauricio Costa for suggesting and motivating the use of ED in this article, and Dr. Paulo Ricardo Batista for their valuable comments and help. This work was funded by the National Research Council of Argentina (CONICET), the Nacional University of La Plata (UNLP) and Carlos Chagas Filho Foundation for Research Support of the Rio de Janeiro State (FAPERJ). YR. Espinosa was supported by the CONICET and FAPERJ; J. R. Grigera is a member of the Research Career of the CONICET, and an Emeritus Professor of the UNLP and E. R. Caffarena is a fellow researcher of the Conselho Nacional de Desenvolvimento Científico e Tecnológico (CNPq).

## REFERENCES

- 1. Luan B, Shan B, Baiz C, Tokmakoff A, Raleigh DP. Cooperative cold denaturation: the case of the C-terminal domain of ribosomal protein L9. Biochemistry 2013;52:2402-2409.
- 2. Privalov PL. Cold denaturation of proteins. Crit Rev Biochem Mol Biol 1990;25:281-305.
- 3. Shan B, McClendon S, Rospigliosi C, Eliezer D, Raleigh DP. The cold denatured state of the C-terminal domain of protein L9 is compact and contains both native and non-native structure. J Am Chem Soc 2010;132:4669-4677.
- 4. Ascolese E, Graziano G. On the cold denaturation of globular proteins. Chem Phys Lett 2008;467:150-153.
- 5. Dias CL, Ala-Nissila T, Wong-ekkabut J, Vattulainen I, Grant M, Karttunen M. The hydrophobic effect and its role in cold denaturation. Cryobiology 2010;60:91-99.
- 6. Adrover M, Esposito V, Martorell G, Pastore A, Temussi PA. Understanding cold denaturation: the case study of Yfh1. J Am Chem Soc 2010;132:16240-16246.
- 7. Adrover M, Martorell G, Martin SR, Urosev D, Konarev PV, Svergun DI, Daura X, Temussi P, Pastore A. The role of hydration in protein stability: comparison of the cold and heat unfolded states of Yfh1. J Mol Biol 2012;417:413-424.
- 8. Pastore A, Martin SR, Politou A, Kondapalli KC, Stemmler T, Temussi PA. Unbiased cold denaturation: low- and hightemperature unfolding of yeast frataxin under physiological conditions. J Am Chem Soc 2007;129:5374-5375.
- 9. Kauzmann W. Some factors in the interpretation of protein denaturation. Adv Protein Chem1959;14:1-63.
- 10. Blokzijl W, Engberts JB. Hydrophobic effects. Opinions and facts. Angew Chem Int Ed Eng 1993;32:1545-1579.
- 11. Dias CL, Ala-Nissila T, Karttunen M, Vattulainen I, Grant M. Microscopic mechanism for cold denaturation. Phys Rev Lett 2008;
- 12. Chara O, McCarthy AN, Grigera JR. Crossover between tetrahedral and hexagonal structures in liquid water. Phys Lett A 2010;375:572-576.
- 13. Fanetti S, Lapini A, Pagliai M, Citroni M, Di Donato M, Scandolo S, Righini R, Bini R. Structure and dynamics of low-density and highdensity liquid water at high pressure. J Phys Chem Lett 2014;5:235-240.
- 14. Royer CA. Revisiting volume changes in pressure-induced protein unfolding. Biochim Biophys Acta 2002;1595:201-209.
- 15. Refaee M, Tezuka T, Akasaka K, Williamson MP. Pressure-dependent changes in the solution structure of hen egg-white lysozyme. J Mol Biol 2003;327:857-865.
- 16. Hinz HJ, Vogl T, Meyer R. An alternative interpretation of the heat capacity changes associated with protein unfolding. Biophys Chemy 1994;52:275-285.
- 17. Dias CL. Unifying microscopic mechanism for pressure and cold denaturations of proteins. Phys Rev Lett 2012;109:048104.
- 18. Chalikian TV, Bresiauer KJ. On volume changes accompanying conformational transitions of biopolymers. Biopolymers 1996;39:619-626.
- 19. He Y, Alam SL, Proteasa SV, Zhang Y, Lesuisse E, Dancis A, Stemmler TL. Yeast frataxin solution structure, iron binding, and ferrochelatase interaction. Biochemistry 2004;43:16254-16262.
- 20. Van Der Spoel D, Lindahl E, Hess B, Groenhof G, Mark AE, Berendsen HJ. GROMACS: fast, flexible, and free. J Comput Chem 2005;26:1701-1718.
- 21. Huang W, Lin Z, van Gunsteren WF. Validation of the GROMOS 54A7 force field with respect to beta-peptide folding. J Chem Theory Comput 2011;7:1237-1243.
- 22. Schmid N, Eichenberger AP, Choutko A, Riniker S, Winger M, Mark AE, van Gunsteren WF. Definition and testing of the GROMOS force-field versions 54A7 and 54B7. Eur Biophys J 2011;40:843-856.
- 23. Abraham MJ, Gready JE. Optimization of parameters for molecular dynamics simulation using smooth particle-mesh Ewald in GRO-MACS 4.5. J Comput Chem 2011;32:2031-2040.

- 24. Hess B, Bekker H, Berendsen HJC, Fraaije JGEM. LINCS: a linear constraint solver for molecular simulations. J Comput Chem 1997; 18:1463-1472.
- 25. Berendsen HJC, Grigera JR, Straatsma TP. The missing term in effective pair potentials. J Phys Chem 1987;91:6269-6271.
- 26. Bussi G, Donadio D, Parrinello M. Canonical sampling through velocity rescaling. J Chem Phys 2007;126:014101.
- 27. Parrinello MAR. Polymorphic transitions in single crystals: a new molecular dynamics method. J Appl Phys 1981;52:7182-7190.
- 28. Maisuradze GG, Liwo A, Scheraga HA. Relation between free energy landscapes of proteins and dynamics. J Chem Theory Comput 2010; 6:583-595.
- 29. Papaleo E, Mereghetti P, Fantucci P, Grandori R, De Gioia L. Freeenergy landscape, principal component analysis, and structural clustering to identify representative conformations from molecular dynamics simulations: the myoglobin case. J Mol Graphics Model 2009;27:889-899.
- 30. Hess B. Convergence of sampling in protein simulations. Physical Review E, Statistical, Nonlinear, and Soft Matter Physics 2002;65: 031910.

- 31. Hess B. Similarities between principal components of protein dynamics and random diffusion. Phys Rev E 2000;62:8438-8448.
- 32. Vega C, Sanz E, Abascal JL. The melting temperature of the most common models of water. The Journal of Chemical Physics 2005; 122:114507.
- 33. Kabsch W, Sander C. Dictionary of protein secondary structure: pattern recognition of hydrogen-bonded and geometrical features. Biopolymers 1983;22:2577-2637.
- 34. Aznauryan M, Nettels D, Holla A, Hofmann H, Schuler B. Singlemolecule spectroscopy of cold denaturation and the temperatureinduced collapse of unfolded proteins. J Am Chem Soc 2013;135: 14040-14043.
- 35. Amadei A, Linssen AB, Berendsen HJ. Essential dynamics of proteins. Proteins 1993;17:412-425.
- 36. Urayama P, Phillips GN, Jr, Gruner SM. Probing substrates in sperm whale myoglobin using high-pressure crystallography. Structure 2002;10:51-60.
- 37. Silva YRE, Grigera JR. Micelle stability in water under a range of pressures and temperatures; do both have a common mechanism? RSC Adv 2015;5:70005-70009.